Title	Complete mode identification for resonance ultrasound spectroscopy
Author(s)	Ogi, Hirotsugu; Sato, Keiji; Asada, Takeyasu et al.
Citation	Journal of the Acoustical Society of America. 2002, 112(6), p. 2553-2557
Version Type	VoR
URL	https://hdl.handle.net/11094/84147
rights	Copyright 2002 Acoustical Society of America. This article may be downloaded for personal use only. Any other use requires prior permission of the author and the Acoustical Society of America.
Note	

Complete mode identification for resonance ultrasound spectroscopy

Hirotsugu Ogi,[a] Keiji Sato, Takeyasu Asada, and Masahiko Hirao
Graduate School of Engineering Science, Osaka University, Machikaneyama 1-3, Toyonaka, Osaka 560-8531, Japan

This study is devoted to deducing exact elastic constants of an anisotropic solid material without using any advance information on the elastic constants by incorporating a displacement-distribution measurement into resonant ultrasound spectroscopy (RUS). The usual RUS method measures free-vibration resonance frequencies of a solid and compares them with calculations to find the most suitable set of elastic constants by an inverse calculation. This comparison requires mode identification for the measured resonance frequencies, which has been difficult and never been free from ambiguity. This study then adopts a laser-Doppler interferometer to measure the displacement-distribution patterns on a surface of the vibrating specimen mounted on pinducers; comparison of the measured displacement distributions with those computed permits us to correctly identify the measured resonance frequencies, leading to unmistakable determination of elastic constants. Because the displacement patterns are hardly affected by the elastic constants, an exact answer is surely obtained even when unreasonable elastic constants are used as initial guesses at the beginning of the inverse calculation. The usefulness of the present technique is demonstrated with an aluminum alloy and a langasite crystal. © *2002 Acoustical Society of America.* [DOI: 10.1121/1.1512700]

I. INTRODUCTION

Resonant ultrasound spectroscopy (RUS)[1–5] has been recognized as a useful method for determining all of the independent elastic constants C_{ij} of an anisotropic solid in a regular shape such as a sphere, cylinder, or rectangular parallelepiped. The C_{ij} are determined in two steps. First, a swept-frequency experiment measures many of the free-vibration resonance frequencies of the specimen. Two transducers touch the specimen lightly, one for generation of a cw oscillation and the other for detection of the displacement amplitude. Second, an inverse calculation is performed to find the best fitting C_{ij} that provide the closest resonance frequencies to the measurements. The resonance frequencies can be calculated using the specimen dimensions, mass density, and all of the C_{ij}.

The successful determination of elastic constants by the RUS method relies on exact correspondence between the observed and calculated resonance frequencies in the inverse calculation, that is, correct mode identification. If modes are incorrectly identified, the elastic constants may converge to a false minimum or fail to converge. However, mode identification has never been straightforward because the measured resonance spectrum contains a large number of resonance peaks, without showing any mode information. On the other hand, the calculation identifies the resonance modes. Thus, if one knows beforehand a set of elastic constants close to the true values, the calculation is highly likely to converge o the correct modes of the specimen. If one begins with very little information about the specimen's C_{ij}, it may not converge

correctly. Several efforts have been made to overcome this difficulty. Ohno[2] noted different rates of changes of resonance frequencies when the specimen size varies. Maynard[6] switched assignments of frequencies during the iteration calculation to find the best fit. Migliori *et al.*[7] changed the specimen orientation relative to the transducers and monitored the change of signal amplitude. More recently, the present authors[8,9] developed an electromagnetic-acoustic technique to select measurable vibration modes by controlling the electromagnetic-force direction. These methods are sometimes useful but still insufficient to make *complete* mode identification. They require supplementing RUS with some other methods such as pulse-echo and rod-resonance methods.

In this study, we propose an advanced methodology for this purpose. We adopt a laser-Doppler velocimeter to map a displacement-distribution pattern of a vibrating specimen. The displacements inside the specimen can be computed. Comparison of the measurements with the computations realizes correct mode identification and then the unmistakable determination of elastic constants.

II. DISPLACEMENT MEASUREMENT AT RESONANCE

Figure 1 shows the measurement setup of the RUS/Laser combination. A rectangular-parallelepiped specimen is put on a piezoelectric tripod consisting of two pinducers for generation and detection of vibration, and one for support. A He–Ne laser beam is focused on the specimen surface (focal diameter: 15 μm) to scan the surface. The reflected beam enters the Doppler interferometer, which measures the nor-

---
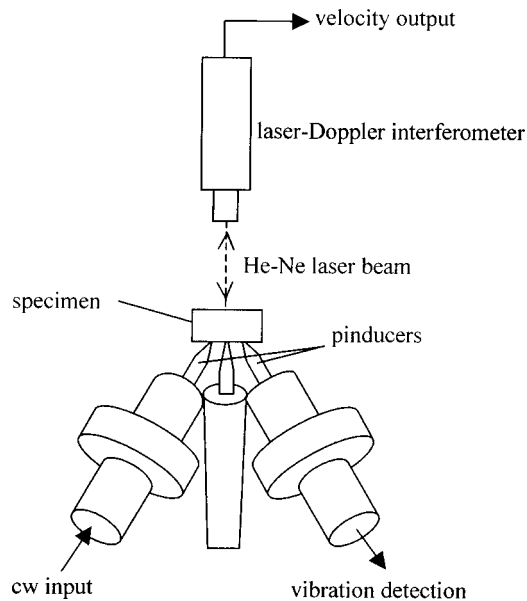[a]Electronic mail: ogi@me.es.osaka-u.ac.jp

FIG. 1. RUS/Laser measurement setup.

mal component of the velocity at the focal point. The velocity is easily converted into the displacement because of harmonic oscillation.

First, we sweep the driving frequency to obtain the resonance spectrum as shown in Fig. 2 and measure the resonance frequencies by fitting a Lorentzian function around the peaks. The contact between the specimen and pinducers is weak and stable because only the specimen mass contributes to the acoustic coupling between the pinducers and specimen, which ensures high reproducibility in the resonance-frequency measurements. (Scattering of a measured resonance frequency was less than 10^{-4}.)

Second, we drive one of the pinducers at a measured resonance frequency while scanning the specimen surface with the laser-Doppler interferometer to acquire the displacement distribution. The signal-to-noise ratio can be improved by Fourier-transforming the output signal from the interferometer to extract the component at the same frequency as the driving cw signal.

This RUS/Laser technique functioned for specimens with a mass larger than 0.01 g, with a surface area larger than 2 mm-by-2 mm square, and with a Q^{-1} value smaller than 10^{-3}. Typical time needed to measure and display a displacement figure was 1 min.
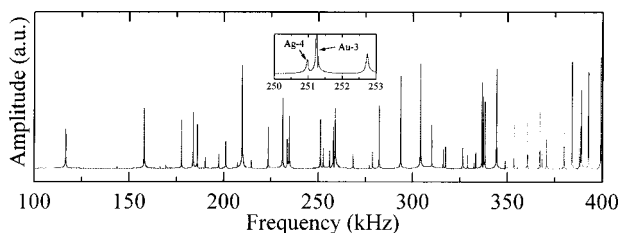

FIG. 2. Resonance spectrum measured by the pinducers for the aluminum alloy specimen. Only the specimen mass contributed to the dry acoustic coupling.

III. CALCULATION OF DISPLACEMENT DISTRIBUTION

No analytical solution exists for the displacements in a rectangular-parallelepiped solid subjected to a free vibration. Thus, the displacements have been approximated by linear combinations of basis functions, and the Rayleigh–Ritz approach has been adopted to determine the accompanying coefficients. Demarest[1] showed that use of normalized Legendre functions as basis functions result in an accurate description of the displacements of a cube specimen with a minimum number of terms. Ohno[2] applied a basis of Legendre functions to describe the displacements of a rectangular-parallelepiped specimen and established the calculation of the free-vibration resonance frequencies. We follow them in this study.

The displacement u_i along the x_i direction can be approximated as

$$u_i(x_1,x_2,x_3) = \sum_k a_k^{(i)} \Psi_k^{(i)}(x_1,x_2,x_3), \qquad (1)$$

$$\Psi_k^{(i)}(x_1,x_2,x_3) = \sqrt{\frac{8}{L_1 L_2 L_3}} \bar{P}_l(2x_1/L_1)$$
$$\times \bar{P}_m(2x_2/L_2)\bar{P}_n(2x_3/L_3), \qquad (2)$$

in a Cartesian coordinate system. $\bar{P}_\lambda$ denotes the normalized Legendre polynomial of degree λ and L_i denotes the edge length along the x_i axis of the rectangular parallelepiped. Lagrangian minimization[1–7] determines the free-vibration resonance frequencies and the coefficients $a_k^{(i)}$. The resonance frequencies have been compared with the measurements and the inverse calculation based on a least-squares fitting has inferred the C_{ij}.

There are eight vibration groups in the free vibration modes of a rectangular parallelepiped with orthorhombic symmetry, labeled as A_u, A_g, B_{1g}, B_{2g}, B_{3g}, B_{1u}, B_{2u}, and B_{3u} by Mochizuki.[10] Because the calculation of the resonance frequencies is independently performed for each vibration group, we exactly know the group and overtone order of the individual calculated frequencies, that is, we can completely identify them. On the other hand, the measured resonance frequencies never inform us of the mode information. Thus, incorrect comparison between the calculations and measurements, or mode misidentification, has easily occurred in the usual RUS method unless excellent initial guesses are adopted.

We pay attention to the coefficients $a_k^{(i)}$ to make correct mode identification. They tell us the two-dimensional pattern of the oscillating specimen surface, which is a *signature* of the individual mode. Thus, the correspondence between the measured and computed displacement distributions guarantees correct mode identification.

IV. RESULTS AND DISCUSSIONS

A. Polycrystalline aluminum alloy

First, we demonstrate the capability of the present technique with a polycrystalline aluminum alloy. The specimen measures $L_1 = 11.92$ mm, $L_2 = 10.93$ mm, and $L_3 = 9.86$ mm and has mass density 2788 kg/m³. We assume isotropic elas-

(a) A_g-4 (250.98 kHz)   (c) B_{1g}-5 (336.65 kHz)

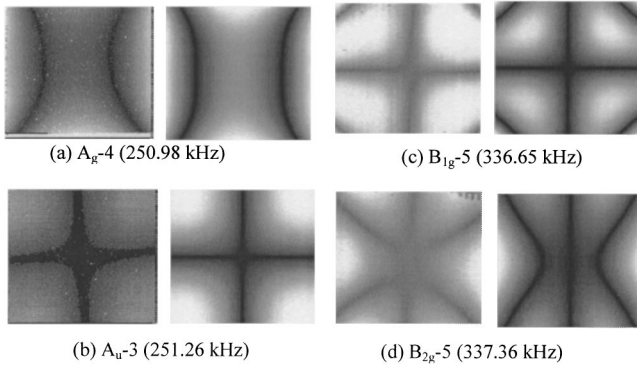(b) A_u-3 (251.26 kHz)   (d) B_{2g}-5 (337.36 kHz)

FIG. 3. Comparison of the distribution of the normal displacement amplitude between measurements (left) and computations (right) for the aluminum alloy rectangular parallelepiped. The x_1 and x_2 axes are along the horizontal and vertical directions, respectively. The origin is located at the center of the rectangular parallelepiped.

TABLE I. Measured (f_{meas}) and calculated (f_{calc}) resonance frequencies (kHz) after convergence for the aluminum alloy rectangular parallelepiped. Mode notation follows Mochizuki (Ref. 10). The average difference of $f_{meas} - f_{calc}$ was 0.2%.

Mode	f_{meas}	f_{calc}	Diff. (%)
A_u-1	116.716	116.32	0.33
A_u-2	143.783	143.186	0.41
$B_{1u}-1$	158.081	158.44	-0.22
$B_{2u}-1$	166.5	166.113	0.23
$B_{1g}-1$	169.523	169.338	0.11
$B_{2g}-1$	177.846	178.36	-0.29
$B_{3u}-1$	183.875	184.57	-0.38
$B_{3g}-1$	186.047	185.078	0.52
A_g-1	190.341	190.206	0.07
$B_{1u}-2$	197.386	197.692	-0.15
A_g-2	201.133	201.462	-0.16
$B_{3g}-2$	207.386	207.096	0.14
A_g-3	209.836	211	-0.56
$B_{2g}-2$	214.753	215.613	-0.40
$B_{2u}-2$	223.548	223.219	0.14
$B_{3u}-2$	231.266	230.804	0.20
$B_{3g}-3$	233.538	233.329	0.09
$B_{1g}-2$	234.717	234.758	-0.01
A_g-4	250.98	250.777	0.08
A_u-3	251.256	251.038	0.08
$B_{2g}-3$	252.742	252.303	0.17
$B_{1u}-3$	256.122	256.849	-0.28
$B_{3u}-3$	257.595	258.064	-0.18
A_g-5	258.118	258.874	-0.29
$B_{2u}-3$	259.035	259.203	-0.06
$B_{1g}-3$	268.54	267.746	0.29
$B_{2u}-4$	277.113	276.736	0.13
$B_{3u}-4$	278.762	279.144	-0.13
$B_{1u}-4$	282.311	282.773	-0.16
$B_{3u}-5$	293.686	293.016	0.22
$B_{2u}-5$	304.159	304.593	-0.14
$B_{1u}-5$	304.464	305.316	-0.27
$B_{1u}-6$	310.109	309.591	0.16
$B_{1g}-4$	316.197	315.775	0.13
$B_{2g}-4$	317.392	317.931	-0.16
A_u-4	326.462	326.556	-0.02
$B_{3g}-4$	329.034	329.369	-0.10
A_g-6	332.441	332.732	-0.08
$B_{2u}-6$	333.364	332.271	0.32
$B_{1g}-5$	336.65	336.218	0.12
$B_{2g}-5$	337.359	337.511	-0.04
A_g-7	338.276	337.71	0.16

tic symmetry and two independent elastic constants C_{11} and C_{44}. Figure 2 shows the resonance spectrum measured by the piezoelectric tripod; many peaks appear and some of them overlap with each other. Thus, it is very difficult, as usual, to identify the modes without advance knowledge of the elastic constants. Figure 3 shows a comparison between the measured and computed displacement-distribution patterns. The computations used arbitrary elastic constants of $C_{11}=100$ and $C_{44}=20$ GPa. Bright regions represent high amplitude displacements and dark regions represent low amplitude displacements; black means zero amplitude, the nodal lines. Typical maximum displacement was a few nm in magnitude. [We call these figures *modern Chladni figures* after Ernst F. F. Chladni (1756–1827), who visualized the resonance oscillations of a square brass plate by putting fine sand on it.[11]] We see very good agreement between the measurements and computations. The usefulness is remarkable, especially in identifying overlapping modes. For instance, the A_g-4 and A_u-3 resonances, indicated by arrows in Fig. 2, occur at very close frequencies (only 0.1% difference) and it is hard to identify them. But, their displacement patterns are quite different from each other [Figs. 3(a) and (b)] and we can straightforwardly distinguish between them. Thus, by identifying all the observed modes (more than 80 now), we determined the C_{ij} via the inverse calculation. Table I shows the measured and calculated resonance frequencies after convergence. Owing to the complete mode identification, there are no missed or extra modes in the measurement. The *exact* elastic constants are $C_{11}=109.26$ and $C_{44}=26.72$ GPa. We tried to deduce the C_{ij} using the usual RUS approach with the initial set of C_{ij} used to compute the displacements in Fig. 3, and pairing the closest resonance frequencies from the measurements and calculations. The inverse calculation failed to converge, indicating that the usual RUS method is sensitive to the initial guesses.

Particularly significant is that the displacement-distribution patterns are insensitive to the elastic constants. In Fig. 4, we show the computed patterns for three cases; (I) isotropic symmetry with the exact C_{ij}; (II) isotropic symmetry with the C_{ij} far away from the exact values; and (III) orthorhombic symmetry with arbitrary nine components of

C_{ij}. Despite the quite different C_{ij}, elastic symmetry, and accordingly resonance frequencies, the resemblance among the resultant patterns is striking, especially for the fundamental modes of the eight vibration groups. After all, such an oscillation pattern, or Chladni figure, is governed by the deformation symmetry allowed in the specimen. In the A_u-group vibrations, for example, the x_3 component of displacement, u_3, occurs only when it is an odd function of x_1 and x_2.[2] Therefore, the Chladni figures on the x_3 face of this group always contain odd numbers of nodal lines running along each of the x_1 and x_2 axes. The fundamental mode, therefore, contains the cross-shaped node signature for every case. As for the B_{3g} group, u_3 must be an even function of x_1 and an odd function of x_2, so that the fundamental-mode Chladni figure shows one center nodal line along the x_1 axis; and so forth on. Thus, a Chladni figure is not directly related to the elastic constants. Note that the overtone order is not
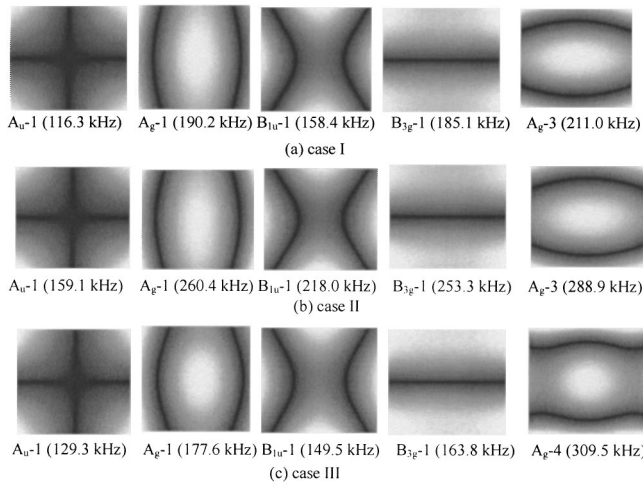
A_u-1 (116.3 kHz) A_g-1 (190.2 kHz) B_{1u}-1 (158.4 kHz) B_{3g}-1 (185.1 kHz) A_g-3 (211.0 kHz)

(a) case I

A_u-1 (159.1 kHz) A_g-1 (260.4 kHz) B_{1u}-1 (218.0 kHz) B_{3g}-1 (253.3 kHz) A_g-3 (288.9 kHz)

(b) case II

A_u-1 (129.3 kHz) A_g-1 (177.6 kHz) B_{1u}-1 (149.5 kHz) B_{3g}-1 (163.8 kHz) A_g-4 (309.5 kHz)

(c) case III

FIG. 4. Displacement-distribution patterns on the x_3 face for three cases: (a) isotropic symmetry with $C_{11} = 109.26$ and $C_{44} = 26.72$ GPa; (b) isotropic symmetry with $C_{11} = 300$ and $C_{44} = 50$ GPa; and (c) orthorhombic symmetry with $C_{11} = 100$, $C_{22} = 150$, $C_{33} = 200$, $C_{12} = 70$, $C_{13} = 60$, $C_{23} = 50$, $C_{44} = 20$, $C_{55} = 30$, and $C_{66} = 40$ GPa. The x_1 and x_2 axes are along the horizontal and vertical directions, respectively. The origin is located at the center of the rectangular parallelepiped.

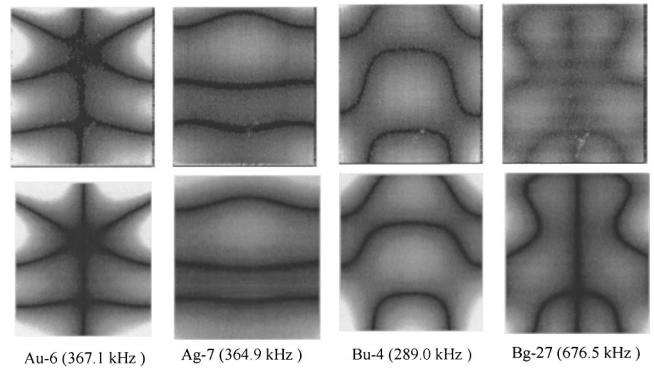Au-6 (367.1 kHz) Ag-7 (364.9 kHz) Bu-4 (289.0 kHz) Bg-27 (676.5 kHz)

FIG. 5. Comparison of the displacement-distribution patterns on the x_3 face of the monocrystal langasite between measurements (upper) and computations (below). The x_1 and x_2 axes are along the horizontal and vertical directions, respectively. The origin is located at the center of the rectangular parallelepiped.

necessarily the same because the C_{ij} affects the resonance frequencies to a large extent; for example, the Chladni figure for the third overtone of A_g group ($A_g - 3$) in cases I and II appears at the fourth overtone in case III (see Fig. 4).

The mode-identification procedure thus becomes an easy task with this technique. Indeed, even unrealistic initial values of $C_{11} = 300$ and $C_{44} = 50$ GPa allowed us to make the complete mode identification and to reach the correct answer.

B. Monocrystal langasite ($La_3Ga_5SiO_{14}$)

We applied this method to a transparent material, monocrystal langasite, by depositing a reflective thin film on the surface. Langasite is a candidate material for surface-acoustic-wave filters owing to its large piezoelectric coefficients e_{ij} and nearly temperature-independent elastic constants. The langasite's crystal structure belongs to the trigonal system with point group 32, thus involving six independent C_{ij}, two e_{ij}, and two dielectric coefficients κ_{ij}. All of them affect the free vibration, which means that e_{ij} and κ_{ij} can be determined by the RUS method together with the C_{ij}.

We used a rectangular parallelepiped crystal with dimensions of $L_1 = 8.027$ mm, $L_2 = 9.804$ mm, and $L_3 = 6.029$ mm. The mass density was 5725 kg/m^3. We deposited a 100-nm-thick aluminum film on the surface normal to the x_3 axis (the three-fold axis of the trigonal system). The free-vibration modes for trigonal symmetry fall into the four groups of A_u, A_g, B_u, and B_g.[10] The Legendre basis functions in Eq. (2) are again available not only to describe the displacements but also to describe the electric potential. The detailed calculation procedure has been given by Ohno.[12]

We see excellent agreement between the measured and computed Chladni figures (Fig. 5). The crystal's elastic anisotropy causes asymmetric patterns about the x_1 axis (the two-fold axis). We could identify more than 80 observed resonance peaks, that is, up to more than 20 overtones in

each group. Thus, the determination of all the material coefficients may be possible and we intend to report on this effort in near future.

V. CONCLUSIONS

We reached the following conclusions from this study.

(1) The RUS/Laser method presented here enables us to identify all observed vibration modes of a rectangular parallelepiped. This leads us to the exact elastic constants, removing the uncertainty in mode identification that has always troubled us.

(2) The displacement-distribution patterns are hardly affected by the elastic constants and elastic symmetry. Therefore, by comparing the measured and computed displacement patterns, we can obtain exact elastic constants with initial guesses far away from the truth. Even the initial values more than 200% different from the correct values resulted in the exact answer.

(3) The present technique also applies to a transparent material with a reflective thin film deposited on the specimen surface. This was demonstrated using a monocrystal langasite.

ACKNOWLEDGMENTS

[1] H. Demarest, Jr., "Cube resonance method to determine the elastic constants of solids," J. Acoust. Soc. Am. **49**, 768–775 (1971).

[2] I. Ohno, "Free vibration of a rectangular parallelepiped crystal and its application to determination of elastic constants of orthorhombic crystals," J. Phys. Earth **24**, 355–379 (1976).

[3] J. Maynard, "Resonant ultrasound spectroscopy," Phys. Today **49**, 26–31 (1996).

[4] A. Migliori and J. Sarrao, *Resonant Ultrasound Spectroscopy* (Wiley, New York, 1997).

[5] H. Ledbetter, C. Fortunko, and P. Heyliger, "Orthotropic elastic constants of a boron–aluminum fiber-reinforced composite: An acoustic-resonance-spectroscopy study," J. Appl. Phys. **78**, 1542–1546 (1995).

[6] J. Maynard, "The use of piezoelectric film and ultrasound resonance to

determine the complete elastic tensor in one measurement," J. Acoust. Soc. Am. **91**, 1754–1762 (1992).

[7] A. Migliori, J. Sarrao, M. W. Visscher, T. Bell, M. Lei, Z. Fisk, and R. Leisure, "Resonant ultrasound spectroscopy techniques for measurement of the elastic moduli of solids," Physica B **183**, 1–24 (1993).

[8] H. Ogi, H. Ledbetter, S. Kim, and M. Hirao, "Contactless mode-selective resonance ultrasound spectroscopy: Electromagnetic acoustic resonance," J. Acoust. Soc. Am. **106**, 660–665 (1999).

[9] H. Ogi, K. Takashima, H. Ledbetter, M. L. Dunn, G. Shimoike, M. Hirao, and P. Bowen, "Elastic constants and internal friction of an SiC-fiber-reinforced Ti-alloy-matrix crossply composite: Measurement and theory," Acta Mater. **47**, 2787–2796 (1999).

[10] E. Mochizuki, "Application of group theory to free oscillations of an anisotropic rectangular parallelepiped," J. Phys. Earth **35**, 159–170 (1987).

[11] C. Taylor, *The Art and Science of Lecture Demonstration* (IOP, Bristol, 1995).

[12] I. Ohno, "Rectangular parallelepiped resonance method for piezoelectric crystals and elastic constants of alpha-quartz," Phys. Chem. Miner. **17**, 371–378 (1990).